Academic Science Journal

Formation of Quaternary Czt(S,Se) Compounds Using Hydrothermal Synthesis and Spin Coating Technique

Ali T. Abbood[*1], Nabeel A. Bakr[1], Falah I. Mustafa[2]

[1] Department of Physics, College of Science, University of Diyala,

[2] Renewable Energy Directorate, Ministry of Science and Technology

talibali98.at@gmail.com

Received: 2 November 2022 **Accepted: 29 January 2023**

DOI: https://doi.org/10.24237/ASJ.02.01.714C

Abstract

$Cu_2ZnSn(Se,S)_4$ or CZT(S,Se) composed of copper, zinc, tin, sulfur, or selenium are developing as promising new long-term light absorption materials for photovoltaic (PV) systems. The materials are abundant, non-toxic, and inexpensive. CZT(S,Se) thin films have been prepared using a two-step procedure. The initial step started with the preparation of CZT(S,Se) powder using the hydrothermal technique which was heat-treated at annealing temperatures of 400°C, 600°C, and 800°C, whereas the second step is the fabrication of CZT(S,Se) thin films using a spin coating process. The XRD result showed that the crystal structure of all films was polycrystalline kesterite phase. At 800 °C, CZTS and CZTSe thin films crystallite size was 15.47 nm and 25.4 nm respectively. According to AFM results, particle size and (RMS) of CZT(S,Se) film increased with increasing annealing temperature when the grain size is directly associated with temperature. The morphological properties using FE-SEM showed that the CZT(S,Se) thin films were compact with more densely packed grains at the highest annealing temperature. The direct band gaps for CZTS and CZTSe estimated by Tauc's equation were (1.73 and 1.68) eV; (1.66 and 1.59) eV; (1.56 and 1.53) eV at 400 °C, 600 °C, and 800 °C respectively. The energy gap of CZT(S,Se) materials is not far off the optimum value for the greatest solar cell efficiency. Hall measurements revealed that all of the samples were p-type.

Academic Science Journal

The lowest value of resistivity was found to be 0.031 Ω.cm for CZTS at 800°C and 0.0191 Ω.cm for CZTSe at the same annealing temperature.

Keywords: CZT(S,Se); Hydrothermal synthesis; Spin coating technique; Thermal annealing .

تكوين المركبات الرباعية CZT (S,Se) المحضر بتقنية التخليق الحراري المائي وتقنية الطلاء الدوراني

علي طالب عبود[1]* و نبيل علي بكر[1] و فلاح ابراهيم مصطفى[2]

[1] قسم الفيزياء ، كلية العلوم ، جامعة ديالى

[2] مديرية الطاقة المتجددة ، وزارة العلوم والتكنولوجيا

الخلاصة

ان المركبات $Cu_2ZnSn(Se,S)_4$ الرباعية تتكون من النحاس والزنك و القصدير والكبريت أوالسيلينيوم، يتم تطويرها باعتبارها مواد جديدة واعدة لامتصاص الضوء على المدى الطويل للأنظمة الكهروضوئية (PV). هذه المواد متوفرة بكثرة وغير سامة، وغير مكلفة. في هذا العمل تم تحضير أغشية CZT(S,Se) الرقيقة باستعمال خطوتين، بدأت الخطوة الأولى بتحضير مسحوق CZT(S,Se) باستعمال التقنية الحرارية المائية التي تمت معالجتها عند درجات حرارة تلدين 400 و 600 و 800 درجة سيليزية، بينما الخطوة الثانية هي تصنيع أغشية CZT(S,Se) الرقيقة باستعمال تقنية الطلاء الدوراني. تم استعمال AFM و XRD و FE-SEM لتوصيف العينات. أظهرت نتيجة XRD أن التركيب البلوري لجميع الأغشية كان عبارة عن طور kesterite متعدد التبلور. عند درجة حرارة التلدين 800 درجة سيليزية، كان حجم بلوريات الغشائين CZTS و CZTSe مساوية لـ 15.47 نانومتر و 25.4 نانومتر على التوالي. وفقًا لنتائج AFM، زاد حجم الجسيمات و (RMS) لاغشية CZT (S,Se) مع زيادة درجة حرارة التلدين اذ يرتبط حجم الحبيبات بدرجة الحرارة بشكل طردي. أظهرت الخصائص المورفولوجية باستعمال FE-SEM أن أغشية CZT (S,Se) الرقيقة كانت متراصة مع حبيبات معبأة بشكل أكثر كثافة عند أعلى درجة حرارة تلدين. كانت فجوات الطاقة المباشرة لـ CZTS و CZTSe المقدرة بواسطة معادلة Tauc (1.73 و 1.68) الكترون فولت عند درجة حرارة تلدين 400 درجة سيليزية ؛ (1.66 و 1.59) الكترون فولت عند درجة حرارة تلدين 600 درجة سيليزية؛ (1.56 و 1.53) الكترون فولت عند درجة حرارة تلدين 800 درجة سيليزية ، فجوة الطاقة لاغشية CZT (S,Se) ليست بعيدة عن القيمة المثلى لأكبر كفاءة للخلايا الشمسية. كشفت قياسات هول أن جميع العينات كانت من النوع p-type. أقل قيمة للمقاومية كانت (0.031Ω.cm) لـ CZTS عند 800 درجة سيليزية و(0.00191Ω.cm) لـ CZTSe عند نفس درجة حرارة التلدين.

الكلمات المفتاحية: CZT (S,Se) ؛ التخليق الحراري المائي ؛ تقنية الطلاء الدوراني ؛ التلدين الحراري.

Academic Science Journal

Introduction

Copper zinc tin sulfide or selenide CZT(S,Se) materials have attracted the interest of many scientists as new and light absorber materials for film solar cell applications. CZT(S,Se) has optical and electronic properties that are advantageous in thin-film solar cells applications, as well as being composed of abundant, non-toxic elements. $Cu_2ZnSn(S,Se)_4$ based thin-film solar cell manufactured using a hydrothermal technique achieved up to 12% Power conversion efficiency (PCE) [1]. Hydrothermal process, is an inexpensive and environmentally friendly technique [2]. The main advantage of this method is the high crystallinity and high quality materials. The purity of the generated CZT(S,Se) components has always been a difficulty in the non-organic, water-based hydrothermal fabrication technique. The phase diagram of the Cu_2S-SnS-ZnS system demonstrated that a single-phase CZT(S,Se) semiconductor can only be produced in a very small region [3]. This is due to the fact that secondary phases such as $Cu_{2-x}S$, ZnS, SnS_2, and Cu_xSnS_y have a higher probability of developing than CZT(S,Se). Metal oxides are also likely to occur in a hydrothermal system in the absent of chelating agents. These impurities (secondary phases and metal oxides) in the solar cell can act as shunting current paths or recombination centers which lower the solar cell's performance. CZT(S,Se) compounds are gaining great interest as promising new light-absorbing material for solar cell applications. CZT(S,Se) is a direct band p-type semiconductor material of nearly (1.5 eV) and a strong light absorption coefficient in the visible and near-infrared region [4,5]. CZT(S,Se) nanocrystals have been considered as a material for high (PCE) solar technology [6,7]. In present work the preparation and characterization of $Cu_2ZnSn(S,Se)_4$ nanoparticle and thin films compound by using two simple and low cost hydrothermal and spin coating technique.

Experimental

1. Preparing of CZT(S, Se) alloy by hydrothermal technique

1.1 Preparation of CZTS powder

0.114 M $CuCl_2.2H_2O$, 0.06 M $ZnCl_2$, 0.06 M $SnCl_2.2H_2O$ and 0.26 M $Na_2S.9H_2O$ are mixed and dissolved in 100 ml of deionized water. The solution was sonicated for 30 minutes for

complete dissolution. In a 120 mL hydrothermal reactor, the mixture was heated to 230°C for 15 hours. After that, the reactor was cooled down to reach room temperature. A black precipitate is obtained which was then washed with deionized water and ethanol; filtered and separated by centrifuge at 8000 rpm for 15 min. After 2 hours of heating at 80°C, the CZTS powder was formed. Furthermore, the samples were annealed at 400, 600, and 800 °C.

1.2 Preparation of CZTSe powder

0.04 M $CuCl_2$, 0.02 M $Zn(NO_3)_2$, 0.02 M $SnCl_2$, and 0.26 M Se are mixed and dissolved in 100 ml of deionized water. The solution was sonicated for 30 minutes for complete dissolution. In a 120 mL hydrothermal reactor, the mixture was heated to 230°C for 15 hours. After that, the reactor was cooled down to reach room temperature. A brown precipitate is obtained which was then washed with deionized water and ethanol; filtered and separated by centrifuge at 8000 rpm for 15 min. After 2 hours of heating at 80°C, the CZTSe powder was formed. Furthermore, the samples were annealed at 400, 600, and 800 °C.

1.3 Preparation of CZT(S,Se) thin films by spin coating technique

The prepared powder is mixed with ethylene glycol to obtain a colloidal solution at ambient temperature with a powder weight (0.75g) and liquid volume (15ml) [8]. Then, the mixture was mixed for 15 min before being sonicated for 30 min. As a result, the stuck solution was produced. The glass substrate was cleaned with detergent, rinsed thoroughly with deionized water and ethanol, and dried. The stuck solution was placed on the glass substrate with the spin coating (450 rpm). To obtain the desired thickness, the cycle was repeated about 10 times.

Results

1. X-ray diffraction (XRD) analysis of CZT(S,Se) thin film

Figure (1) shows X-ray diffraction (DX-2700 with Cu Kα-radiation) results for CZTS films prepared by hydrothermal method, the annealing for powder were at different temperatures 400,600 and 800 ^{o}C, and spin-coating technique, CZTS thin films have a polycrystalline kesterite phase tetragonal structure. The fundamental diffraction peaks appeared at 2θ

=28.4385º, 32.9830º, 37.927º, 47.2885º, 56.2049º, 69.1769º and 76.3995º are attributed to (112), (221), (211), (303), (008), (040) and (332) planes respectively, which are well-matched the standard card (JCPDS No. 26-0575) [9, 10]. the "2θ" position for the (112) direction shifted to a higher value, whereas at 800 ºC it shifted to a lower value, the reason for this is that the annealing temperature increases, the particle size increases, which reduces the stress of the particles, and this decrease in stress leads to the change of the peak, in addition, a change in the lattice parameter and crystal structure [11].

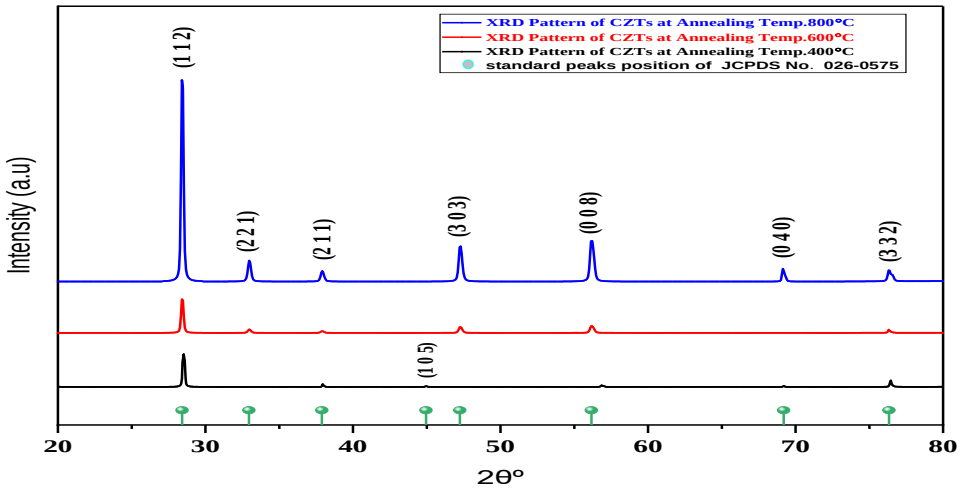

Figure 1: XRD pattern of CZTS thin films, the powder was annealed at different temperatures (400, 600, 800) ºC compared to the reference pattern for kesterite CZTS (JCPDS No. 26-0575)

Figure (2) shows the X-ray diffraction, CZTSe thin films have a polycrystalline kesterite phase tetragonal structure. The fundamental diffraction peaks that appeared at 2θ =21.8105º, 54.1090º and 68.6478º are attributed to (112), (204) and (312) planes respectively, which are well-matched the standard card (JCPDS No.52-0868) [12]. The crystallite size of the CZTSe films increases with the increase in annealing temperature. From the surface morphology, it is observed that the CZTSe films are more uniform and have better crystal structure when annealing temperature increased from 600 °C to 800 °C [13].

Academic Science Journal

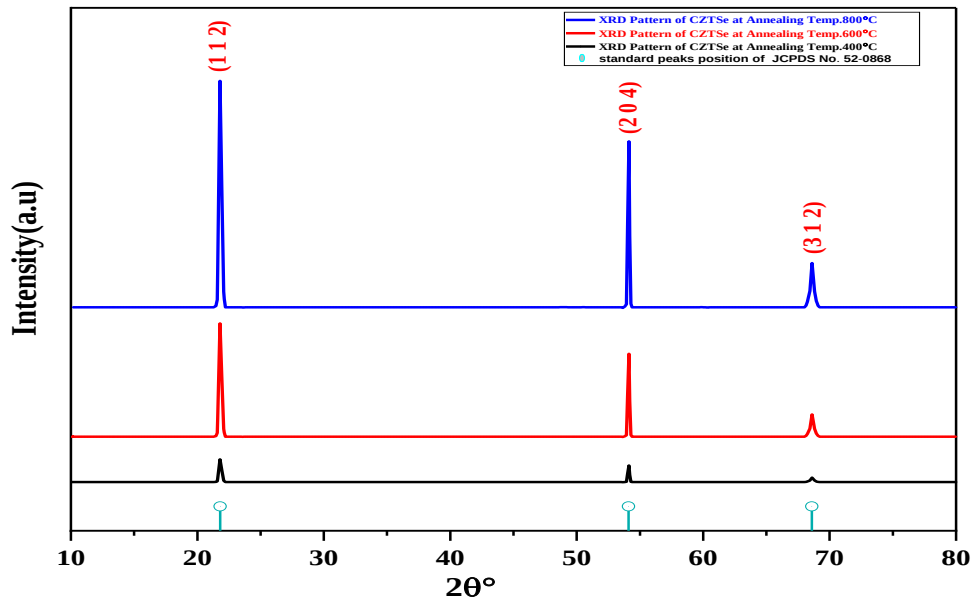

Figure 2: XRD pattern of CZTSe thin films, the powder was annealed at different temperatures (400, 600, 800) ^{o}C compared to the reference pattern for kesterite CZTSe (JCPDS No. 52-0868).

Scherrer's equation can be used to calculate the crystallite size:

$$D = \frac{K\,\lambda}{\beta\,Cos\theta} \qquad \ldots\ldots\ldots\ldots\ldots (1)$$

Where D is the crystallite size, θ is the diffraction angle, β denotes the full width at half maximum of the peak (FWHM) in radians, λ is the incident beam wavelength of 0.15406 nm, and K is the shape factor and its value is close to 0.9. X-RAY diffraction results of prepared CZT(S,Se) thin films, the powder was annealed at different temperatures (400, 600, 800) ^{o}C, see Table (1) , increase in particles size was noticed when the annealing temperature increased. In addition, at an annealing temperature 800 ^{o}C; The lattice constants of CZTS were: a= 5.531Å, c= 10.950Å and for CZTSe were a= 5.432Å, c= 10.734Å (Table (2)). These values were closely related to standard values (a = 5.42 Å) and (c = 10.848Å). The volumes of the unit cell for the above-mentioned compounds samples were smaller than standard volume (326.51 Å^3), due to

stress, the peak intensity increases with decrease in FWHM, the crystallite size of the CZT(S,Se) thin films increases showing the improvement in structural properties of the films. Lattice parameters, a=b of the film increases and c increases with annealing temperatures, the expansion in the volume of the unit cell increases and c/2a ratio is showing the formation of pure kesterite structure of the CZT(S,Se) films [14,15].

Table 1: XRD analysis of $Cu_2ZnSn(S,Se)_4$ at different annealing temperatures with Miller indices (112).

THIN FILM	ANNEALING TEMPERATURE (°C)	2Θ (DEG)	B (DEG)	(HKL)	D (NM)
CZTS	400	28.43859	0.664	112	12.1
	600	28.199	0.423	112	18.8
	800	28.4385	0.401	112	19.9
CZTSe	400	21.742	0.364	112	21.6
	600	22.6384	0.241	112	32.7
	800	21.9421	0.201	112	39.2

Table 2: XRD analysis of $Cu_2ZnSn(S,Se)_4$, the powder was annealed at different temperatures (400, 600, 800) ^oC at (112)plane.

Thin Film	Annealing Temp. (°C)	2θ (deg.)	d (Å)	FWHM (deg.)	D (nm)	Lattice constants a (Å)	c (Å)	c\2a	Unit Cell Volume (Å ^{3})
CZTS	400	28.50	3.1319	0.80	9.5	5.425	10.852	1.001	319.85
	600	28.43	3.1578	0.59	13.8	5.442	10.892	0.98	318.12
	800	28.3	3.1374	0.46	15.4	5.531	10.950	0.97	325.55
CZTSe	400	21.83	3.55	0.45	20.5	5.578	10.790	0.90	303.48
	600	21.80	3.157	0.42	21.2	5.435	10.768	0.96	307.739
	800	21.78	2.941	0.37	25.4	5.432	10.734	0.98	311.052

2. Atomic Force Microscope (AFM)

Figure (3) illustrates the topography of the surface of CZTS thin films at various annealing temperatures (a) 400°C, (b) 600°C, and (c) 800°C. Topography is formed through island development, and kinetic energy is insufficient for the adhesion of island-like crystallites at low temperatures. The root mean square (RMS) surface roughness of the CZTS film at 400°C was

5.160nm. These smaller textured islands adhesion to create the superstructure of smaller clusters with rising RMS surface roughness to 6.982 nm in the CZTS film annealed at 600 °C (Fig. 3b). The island's adhesion could be caused by an increase in surface mobility as the annealing temperature rises. With an increased temperature to 800 °C (Fig. 3(c)), these smaller CZTS clusters are linked together and converted into bigger, non-uniform clusters with high surface roughness, which agrees with the results that have been reported previously [16]. Figure (4) illustrates the AFM images of CZTSe thin films formed at varied temperatures (a) 400°C, (b) 600°C, and (c) 800°C. As a result of the AFM study, it has been determined that as the annealing temperature is increased, the particle size and RMS of the CZT(S,Se) film rises, by AFM images taken at different annealing temperatures of the CZT(S,Se) films. It is observed that film roughness increases as increase in annealing temperature. This is due to increase in grain size with increase in annealing temperatures which agrees with the results that have been reported previously [17]. The CZT(S,Se) films' average roughness and RMS are estimated the number and described in table (3).

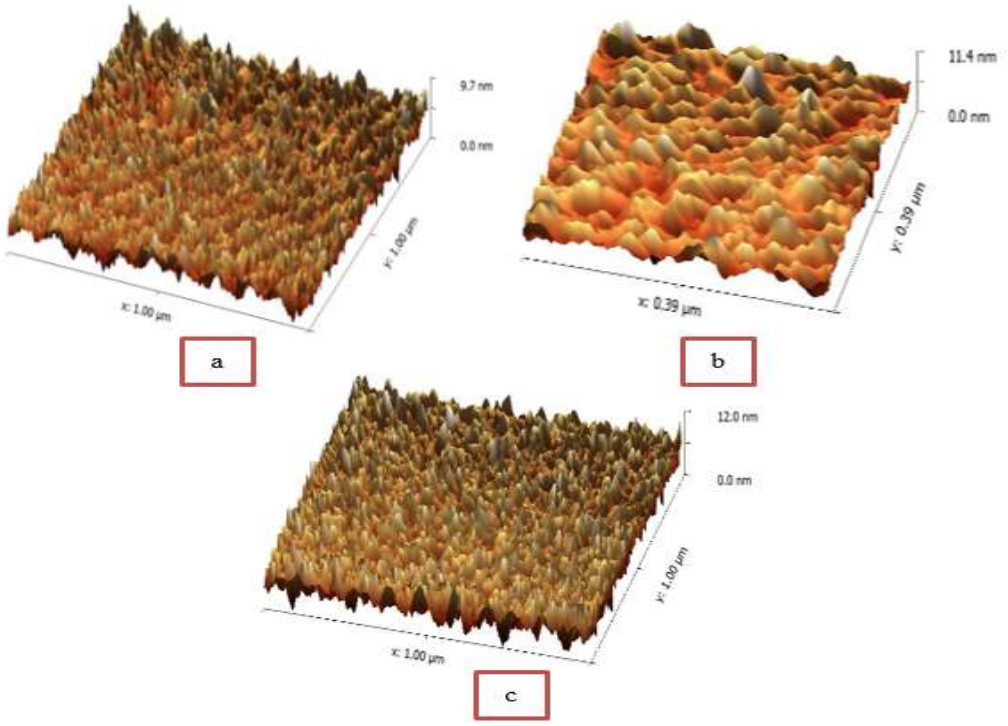

Figure 3: 3-D AFM images of CZTS thin films, the powder was annealed at different temperatures (400, 600, 800) ºC

Academic Science Journal

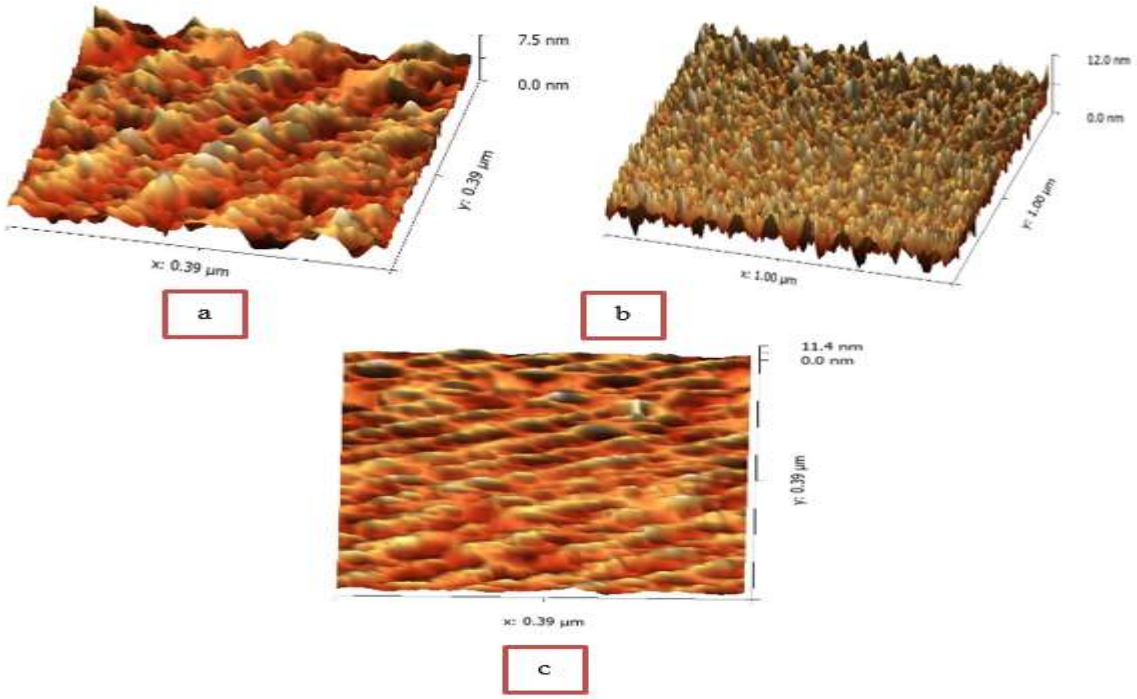

Figure 4: 3-D AFM images of CZTSe thin films, the powder was annealed at different temperatures (400, 600, 800) ºC

Table 3: Surface roughness, root mean square (RMS) surface roughness and grain size of CZTS and CZTSe thin films, the powder was annealed at different temperatures (400, 600, 800) ºC

Thin films	Annealing temperature (°C)	Surface roughness average (nm)	RMS (nm)	Average grain size (nm)
CZTS	400	6.384	5.160	36.83
	600	7.220	6.982	47.54
	800	12.64	9.539	63.21
CZTSe	400	3.61	5.28	25.80
	600	6.89	6.32	44.02
	800	11.52	8.76	52.44

3. Field-emission scanning electron microscopy (FESEM)

Fig. 5(a-c) shows that FE-SEM images of CZTS thin films prepared by hydrothermal, the CZTS powder was annealed at different temperatures 400°C,600°C, and 800°C, and the CZTS films deposited by spin coating, some pores or voids were observed in CZTS film when annealed at 400°C (Fig. 5a). Similarly, annealing the film at 600°C revealed more obvious grain structures and uniform surface morphology (Fig. 5b), the shape of the CZTS films is dependent on annealing temperature and became more compact with more densely packed grains when the annealing rise to 800°C (Fig. 5c) [18].

Fig. 6(a-c) shows FE-SEM images of CZTSe thin films, the grain boundary properties of CZTSe thin films annealed at 400°C and 600°C were sharp (Fig. 6a, b), but grain boundary features of CZTSe thin films annealed at 800°C are smooth. The grains in the CZTSe thin film grown at 800°C are indeed bigger than those produced at 400°C and 600°C. This indicates that grain boundaries are contracting the CZTSe thin film generated at 800°C (Fig. 6c). The particles were semi-spherical and spherical in shape with an average size (89.5 nm, 112.9 nm, and 319.7 nm) for CZTS thin films, And were (96.4 nm, 141.2 nm, and 246.8 nm) for CZTSe thin films, at annealing temperatures (400, 600, 800) ^{o}C respectively, which agrees with the results that have been reported previously [19]. The morphology of this CZT(S,Se) layer, which has a higher density of stacking along back contact, should assist devices in reducing recombination damages and lowering series resistance, which agrees with the results that have been reported previously [20].

Academic Science Journal

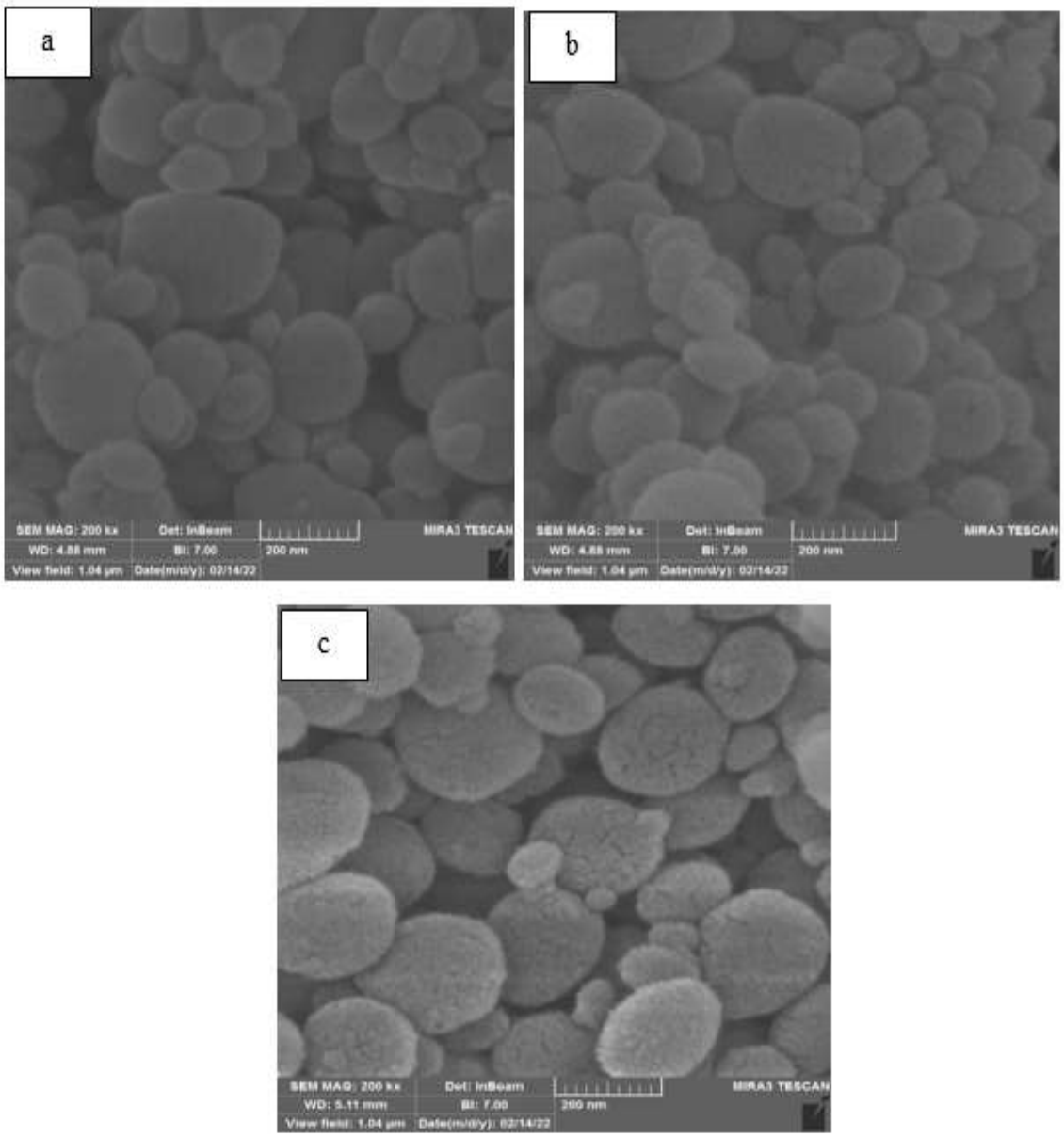

Figure 5: FE-SEM images of CZTS thin, the powder was annealed at different temperatures (a) 400, (b) 600 and (c) 800 °C.

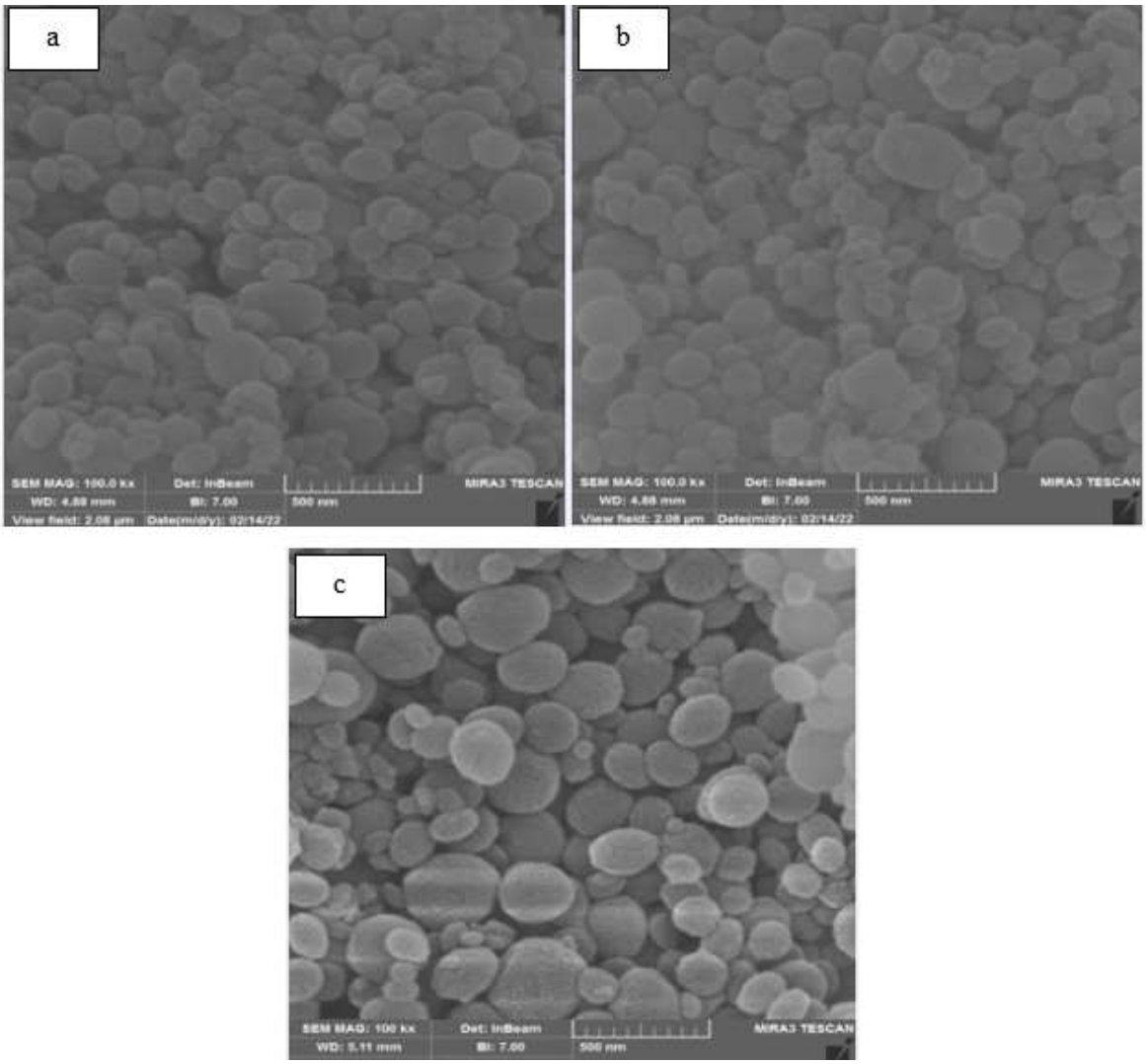

Figure 6: FE-SEM images of CZTSe thin films, the powder was annealed at different temperatures (**a**) 400, (**b**) 600 and (**c**) 800 °C.

4. The Optical Properties

The energy gap of the prepared thin films was calculated from their absorption spectrum using tauc equation:

$$(\alpha h\vartheta) = C(h\vartheta - E_g)^{1\backslash n} \ldots\ldots\ldots\ldots\ldots (2)$$

Where E_g is the energy gap, n is equal to ½ for the direct allowed bandgap, α is the absorption coefficient, and C is a constant depend on the matter nature. The energy gap was calculated using the intercept of the linear part of the plot of $(\alpha h\vartheta)^2$ versus $(h\vartheta)$ with the x-axis (photon

energy axis). The optical band gap of CZTS thin films was obtained as 1.73, 1.66, and 1.56 eV for 400, 600, and 800 ^{o}C respectively as shown in figure 7; this agrees with the results that have been reported [21]. The energy gap of CZTSe thin film was obtained as 1.68, 1.59, and 1.53 eV for 400, 600, and 800 ^{o}C respectively as shown in figure 8; which agrees with the results that have been reported [22]. The optical energy bandgap is decreased with an increase in annealing temperatures, so the narrow bandgap was seen at 800 ^{o}C for CZT(S,Se) thin film, because of that; as the annealing temperature increased, the vacancies increased, which may provide free electrons and enhanced the conductivity of CZT(S,Se) films [23].

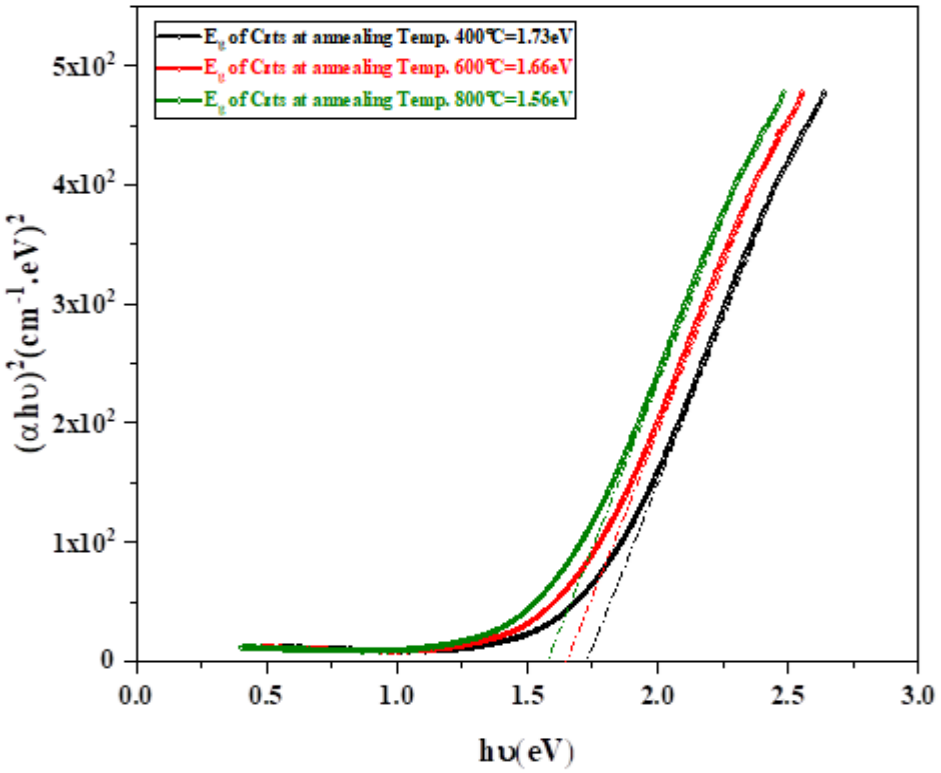

Figure 7: Tauc's plot of CZTS thin film.

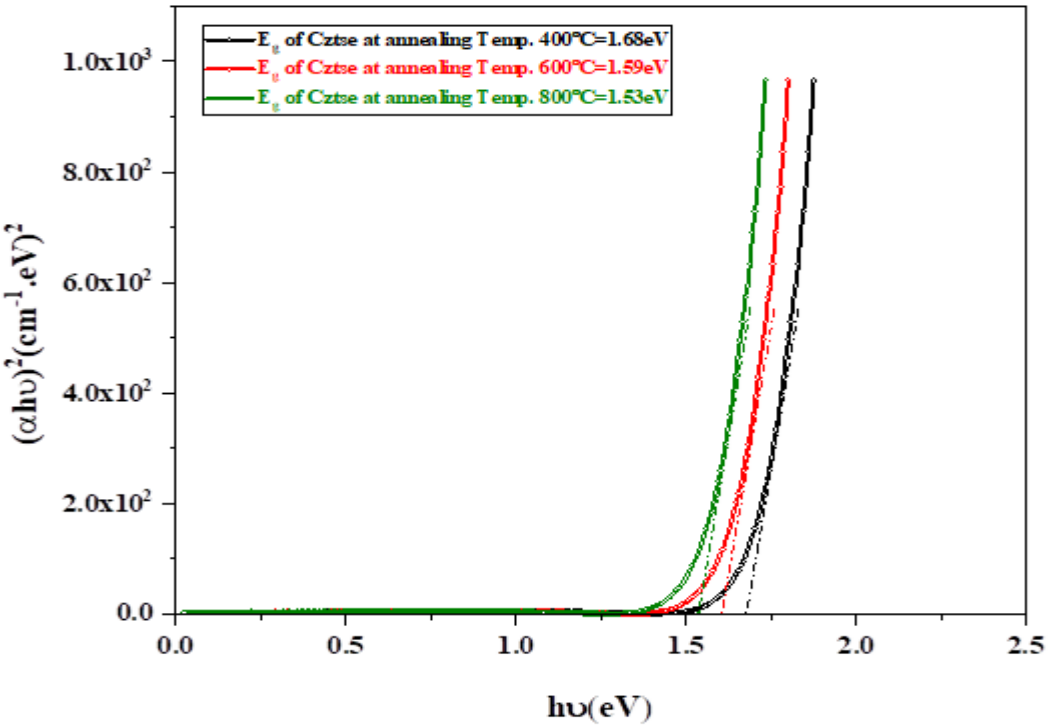

Figure 8: Tauc's plot of CZTSe thin film.

5. Electrical properties

The electrical properties of the quaternary compounds CZT(S,Se) were studied by means of Hall's apparatus, where the mobility, Hall coefficient, resistivity and concentration of charge carriers .All films exhibited p-type conductivity, the highest carrier concentrations were found to be 18.76×10^{17} cm^{-3} for CZTS at 800°C and 20.82×10^{17} $cm^{-3}$for CZTSe at the same temperature, which means that crystal growth has been completed. The low resistivity was found to be 1.1 Ω.cm for CZTS at 800°C and 1. 3 Ω.cm for CZTSe at the same temperature. The range of mobility for CZT(S,Se) films was observed to be 37.25–89.58 $cm^2\ V^{-1}\ s^{-1}$ (Table 4), the mobility rises as the annealing temperature increased, which leads to an increase in the concentration of charge carriers, and consequently, an increase in its electrical conductivity, Also, all the examined samples showed p-type [24]. The electrical conductivity increased with the increasing of annealing temperature, and that led to an increase in the concentration of charge carriers, the reason behind this increase is the occurrence of a more complete

crystallization at high temperature. This was confirmed by the results of the X-ray diffraction, which agrees with the results that have been reported previously [25].

Table 4: Hall Effect properties of CZTS (Se) films, the powder was annealed at different temperatures (400, 600, 800) ^{o}C

Thin film	Annealing temperature (°C)	Resistivity (Ω.cm)	Hall coefficient (cm^3/C)	Carrier concentrations $\times 10^{17}$ cm^{-3}	Hall mobility ($cm^2V^{-1}S^{-1}$)
CZTS	400	1.12	214.3	12.78	37.25
	600	0.014	22.56	15.36	65.32
	800	0.031	20.69	18.76	98.63
CZTSe	400	1.361	32.86	16.85	42.94
	600	0.025	16.59	20.3	46.64
	800	0.0191	32.74	20.82	89.58

Conclusions

CZT(S,Se) thin films have a polycrystalline kesterite phase. the grain size of thin films was increased as the annealing temperature elevated, besides getting a smoother surface for grains, which are essential surface properties for solar cells' efficiency, the shape of the CZT(S,Se) thin films was dependent on the annealing temperature. The electrical conductivity was increased with an increase in the annealing temperature and the concentration of charge carrier also increased, while the resistivity decreased as long as the annealing temperature increased. The optical examinations of CZT(S,Se) thin films have a direct energy gap that is allowed, and the values of energy gaps were decreased since the annealing temperatures increased.

References

1. Wang, W., Winkler, M. T., Gunawan, O., Gokmen, T., Todorov, T. K., Zhu, Y., & Mitzi, D. B. (2014). Device characteristics of CZTSSe thin-film solar cells with 12.6% efficiency. Advanced energy materials, 4(7), 1301465.
2. Taskesen, T., Neerken, J., Schoneberg, J., Pareek, D., Steininger, V., Parisi, J., & Gütay, L. (2018). Device characteristics of an 11.4% CZTSe solar cell fabricated from sputtered precursors. Advanced Energy Materials, 8(16), 1703295.

3. Olekseyuk, I. D., Dudchak, I. V., & Piskach, L. V. (2004). Phase equilibria in the Cu_2S–ZnS–SnS_2 system. Journal of alloys and compounds, 368(1-2), 135-143.
4. Wang, H. (2011). Progress in thin film solar cells based on. International journal of Photoenergy, 2011.
5. Tiong, V. T., Hreid, T., Will, G., Bell, J., & Wang, H. (2014). Polyacrylic acid assisted synthesis of Cu_2ZnSnS_4 by hydrothermal method. Science of Advanced Materials, 6(7), 1467-1474.
6. Guo, Q., Hillhouse, H. W., & Agrawal, R. (2009). Synthesis of Cu_2ZnSnS_4 nanocrystal ink and its use for solar cells. Journal of the American Chemical Society, 131(33), 11672-11673.
7. Zhou, H., Hsu, W. C., Duan, H. S., Bob, B., Yang, W., Song, T. B. & Yang, Y. (2013). CZTS nanocrystals: a promising approach for next-generatio thin film photovoltaics. Energy & Environmental Science, 6(10), 2822-2838.
8. Camara, S. M., Wang, L., & Zhang, X. (2013). Easy hydrothermal preparation of Cu_2ZnSnS_4 (CZTS) nanoparticles for solar cell application. Nanotechnology, 24(49), 495401.
9. Chen, Q. M., Li, Z. Q., Ni, Y., Cheng, S. Y., & Dou, X. M. (2012). Doctor-bladed Cu_2ZnSnS_4 light absorption layer for low-cost solar cell application. Chinese Physics B, 21(3), 038401.
10. Shi, C., Shi, G., Chen, Z., Yang, P., & Yao, M. (2012). Deposition of Cu_2ZnSnS_4 thin films by vacuum thermal evaporation from single quaternary compound source. Materials Letters, 73, 89-91.
11. Zhou, B., Xia, D., & Wang, Y. (2015). Phase-selective synthesis and formation mechanism of CZTS nanocrystals. RSC Advances, 5(86), 70117-70126.
12. Chernomordik, B. D., Béland, A. E., Trejo, N. D., Gunawan, A. A., Deng, D. D., Mkhoyan, K. A., & Aydil, E. S. (2014). Rapid facile synthesis of Cu_2ZnSnS_4 nanocrystals. Journal of Materials Chemistry A, 2(27), 10389-10395.

13. Schorr, S., Weber, A., Honkimäki, V., & Schock, H. W. (2009). In-situ investigation of the kesterite formation from binary and ternary sulphides. Thin Solid Films, 517(7), 2461-2464.
14. Bakr, N. A., Khodair, Z. T., & Mahdi, H. I. (2016). Influence of thiourea concentration on some physical properties of chemically sprayed Cu_2ZnSnS_4 thin films. International Journal of Materials Science and Applications, 5(6), 261-270.
15. Sheleg, A. U., Hurtavy, V. G., Mudryi, A. V., Valakh, M. Y., Yukhymchuk, V. O., Babichuk, I. S., ... & Caballero, R. (2014). Determination of the structural and optical characteristics of Cu_2ZnSnS_4 semiconductor thin films. Semiconductors, 48(10), 1296-1302.
16. Shah, N. M., Panchal, C. J., Kheraj, V. A., Ray, J. R., & Desai, M. S. (2009). Growth, structural and optical properties of copper indium diselenide thin films deposited by thermal evaporation method. Solar Energy, 83(5), 753-760.
17. Kuo, F. Y., Lin, F. S., Yeh, M. H., Fan, M. S., Hsiao, L. Y., Lin, J. J., ... & Ho, K. C. (2019). Synthesis of surfactant-free and morphology-controllable vanadium diselenide for efficient counter electrodes in dye-sensitized solar cells. ACS Applied Materials & Interfaces, 11(28), 25090-25099.
18. Chernov, A. A., & Scheel, H. J. (1995). Extremely flat surfaces by liquid phase epitaxy. Journal of crystal growth, 149(3-4), 187-195.
19. Yao, L., Ao, J., Jeng, M. J., Bi, J., Gao, S., He, Q., ... & Chen, J. W. (2014). CZTSe solar cells prepared by electrodeposition of Cu/Sn/Zn stack layer followed by selenization at low Se pressure. Nanoscale Research Letters, 9(1), 1-11.
20. Paul, S., Lopez, R., Repins, I. L., & Li, J. V. (2018). Study of charge transport properties in a ZnO/CdS/Cu (In, Ga) Se_2 solar cell via admittance spectroscopy. Journal of Vacuum Science & Technology B, Nanotechnology and Microelectronics: Materials, Processing, Measurement, and Phenomena, 36(2), 022904.
21. Bakr, N. A., Khodair, Z. T., & Hassan, S. M. (2015). Effect of substrate temperature on structural and optical properties of Cu_2ZnSnS_4 (CZTS) films prepared by chemical spray pyrolysis method. Research Journal of Chemical Sciences ISSN, 2231, 606X.

22. Wang, W., Winkler, M. T., Gunawan, O., Gokmen, T., Todorov, T. K., Zhu, Y., & Mitzi, D. B. (2014). Device characteristics of CZTSSe thin-film solar cells with 12.6% efficiency. Advanced energy materials, 4(7), 1301465.
23. Chai, Y., Tam, C. W., Beh, K. P., Yam, F. K., & Hassan, Z. (2015). Effects of thermal treatment on the anodic growth of tungsten oxide films. Thin Solid Films, 588, 44-49.
24. Ahmed, H. J., Kamil, A. A., Habeeb, A. A., & Bakr, N. A. (2020). The influence of Deposition Temperature on the Properties of Chemically Sprayed Nanostructured Cu_2CdSnS_4 Thin Films. International Research Journal of Science and Technology, 1(2), 149-155.
25. Al-Shakban, M., Matthews, P. D., Savjani, N., Zhong, X. L., Wang, Y., Missous, M., & O'Brien, P. (2017). The synthesis and characterization of Cu_2ZnSnS_4 thin films from melt reactions using xanthate precursors. Journal of materials science, 52(21), 12761-12771.